Letter

Observation of $\mathcal{PT}$-symmetric quantum coherence in a single-ion system

Wei-Chen Wang,[1,2,*] Yan-Li Zhou,[1,2,*] Hui-Lai Zhang,[3] Jie Zhang,[1,2] Man-Chao Zhang,[1,2] Yi Xie,[1,2] Chun-Wang Wu,[1,2] Ting Chen,[1,2] Bao-Quan Ou,[1,2] Wei Wu,[1,2] Hui Jing,[3,†] and Ping-Xing Chen[1,2,‡]

[1]*Department of Physics, College of Liberal Arts and Sciences, National University of Defense Technology, Changsha 410073, China*

[2]*Interdisciplinary Center for Quantum Information, National University of Defense Technology, Changsha 410073, China*

[3]*Key Laboratory of Low-Dimensional Quantum Structures and Quantum Control of Ministry of Education, and Department of Physics, Hunan Normal University, Changsha 410081, China*

(Received 17 September 2020; revised 20 November 2020; accepted 13 January 2021; published 15 February 2021)

Parity-time ($\mathcal{PT}$)-symmetric systems, featuring real eigenvalues despite their non-Hermitian nature, undergo spontaneous $\mathcal{PT}$ symmetry breaking at the exceptional point (EP). The phase transition from $\mathcal{PT}$ symmetry to $\mathcal{PT}$ symmetry breaking has shown exotic functionalities in the classical realm, such as loss-induced transparency or lasing revival. This transition is also expected to produce a more unconventional effect in pure quantum $\mathcal{PT}$ devices. Here, we report experimental evidences of spontaneous $\mathcal{PT}$ symmetry breaking in a single cold $^{40}Ca^+$ ion and, more importantly, a counterintuitive effect of perfect quantum coherence occurring at the EP. Excellent agreement between experimental results and theoretical predictions is identified. In view of the versatile role of cold ions in building a quantum memory or processor, our experiment provides an alternative platform to explore $\mathcal{PT}$-symmetric physics and utilize pure quantum EP effects.

DOI: 10.1103/PhysRevA.103.L020201

I. INTRODUCTION

In conventional quantum mechanics, Hermiticity is a fundamental axiom ensuring real eigenvalues of physical observables [1]. A striking discovery in recent years has revealed that parity-time($\mathcal{PT}$)-symmetric Hamiltonians [2–4], despite their non-Hermitian nature, can also have real eigenvalues [5,6]. By continuously tuning parameter values, spontaneous $\mathcal{PT}$ symmetry breaking can occur at an exceptional point (EP) [7,8], where both the eigenvalues and the eigenstates of the system coalesce. As a result, many counterintuitive phenomena [9–15] emerge in such systems, e.g., single-mode lasing or antilasing [16,17], loss-induced transparency or lasing [18,19], an EP-enhanced sensing [20,21], to name only a few. These seminal experiments, however, have been performed mainly in the classical realm, and more exotic effects are expected to occur in pure quantum $\mathcal{PT}$ devices.

Achieving $\mathcal{PT}$ symmetry, in principle, requires an exact balance of gain and loss, which is challenging in the quantum realm, since practical systems can be unstable in the presence of gain-amplified noises [22,23]. To overcome this obstacle, passive devices with hidden $\mathcal{PT}$ symmetry were proposed by coupling Hermitian systems to a dissipative reservoir [18,19]. The emergence of EPs in such lossy devices, without any active gain, has been demonstrated in very recent experiments using optical or solid-state systems [24,25], opening up a practical route to observe and manipulate quantum EP effects [24,25]. For an example, quantum coherence protection was observed in a $\mathcal{PT}$-broken superconducting circuit [25], with postselection of the experimental results and an exponentially decreasing success rate for longer times. These pioneering experiments on quantum EP systems [22,24,25] have provided the important first steps towards emerging non-Hermitian quantum technologies.

In this paper we report an experiment on spontaneous breaking of $\mathcal{PT}$ symmetry occurring in a single $^{40}Ca^+$ ion. We note that trapped cold ions having a coherence time as long as 10 min [26] have been widely used for quantum memory [27–29], quantum state preparation [30], quantum simulation [31–34], and high-precision metrology [35,36], and are viewed as powerful candidates for building quantum computers. However, to date, experimental realization of $\mathcal{PT}$ symmetry in such a typical system has not been achieved, hindering its applications in non-Hermitian quantum control of ions. Here we fill this gap by demonstrating clear signatures of the quantum EP in a $^{40}Ca^+$ ion. We deterministically demonstrate EP features by measuring the ion-state populations both in the $\mathcal{PT}$-symmetric (PTS) regime and in the $\mathcal{PT}$-broken (PTB) regime. Furthermore, we observe a turning point of the nondiagonal elements of the density matrix by approaching the EP, due to which giant enhancement of quantum coherence [37] can be achieved for the system. Our paper, as a demonstration of single-ion $\mathcal{PT}$ symmetry breaking, provides an alternative platform to explore and utilize more truly quantum EP effects with applications in quantum engineering of trapped ions.

II. $\mathcal{PT}$ PHASE TRANSITION IN TRAPPED ION SYSTEM

The experimental setup of the trapped $^{40}Ca^+$ ion, with its energy levels, is shown in Figs. 1(a)–1(c). The ion, initially

*These authors contributed equally to this work.
†jinghui73@foxmail.com
‡pxchen@nudt.edu.cn

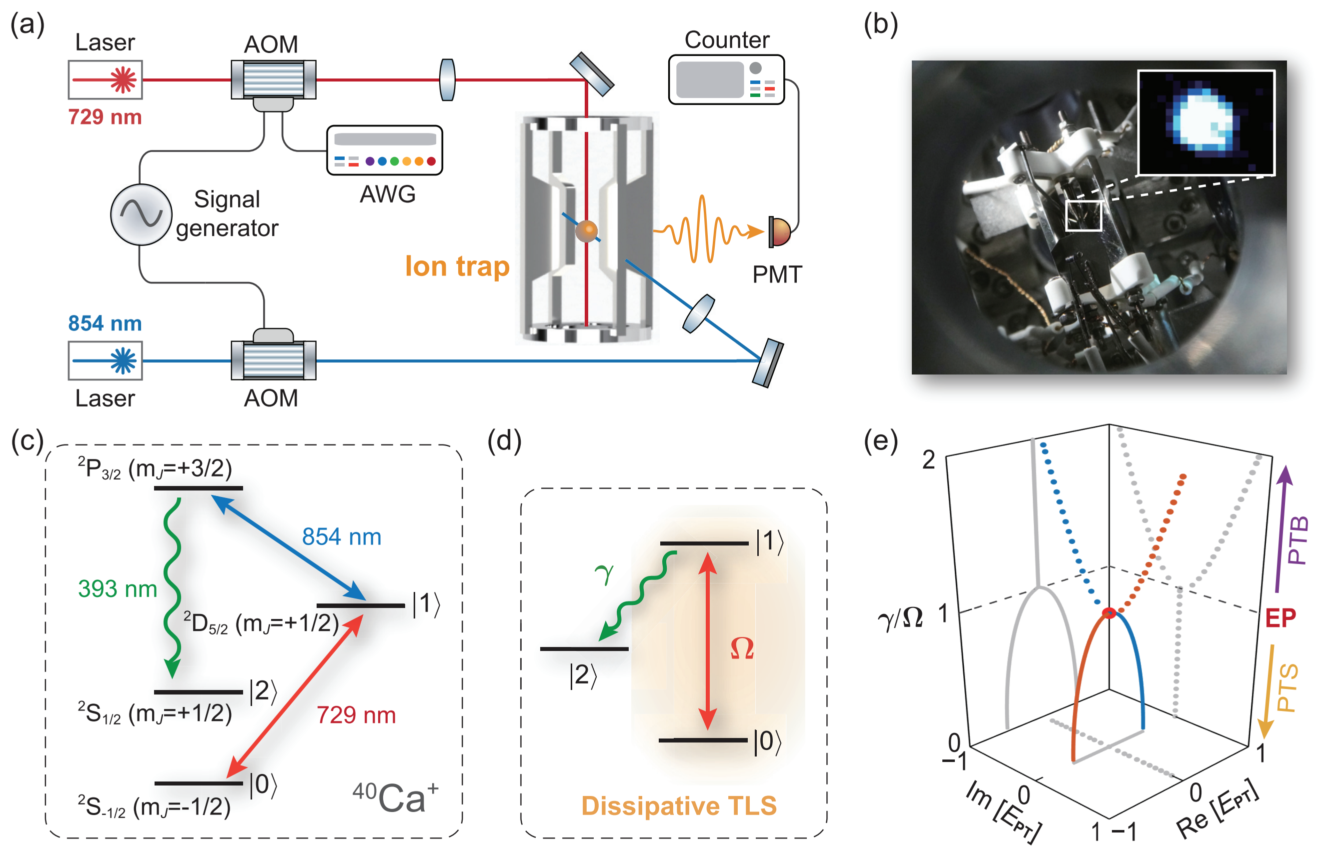

FIG. 1. The experimental system of a passive $\mathcal{PT}$-symmetric single ion. (a) Schematic diagram of the experimental setup. In the experiment, both 729- and 854-nm laser beams are switched on at the same time, and the quantum states of the ion at different times are read out by the electron shelving. Here, AOM denotes the acousto-optical modulator, PMT is the photomultiplier tube, and AWG is the arbitrary waveform generator. (b) The photograph of the ion trap. (c, d) The energy levels of the $^{40}Ca^+$ ion, with the internal states $|0\rangle$, $|1\rangle$, and $|2\rangle$ corresponding to the energy levels $^2S_{1/2}(m_J=-1/2)$, $^2D_{5/2}(m_J=+1/2)$, and $^2S_{1/2}(m_J=+1/2)$, respectively. (e) The eigenvalues of $H_{\mathcal{PT}}$ vs γ/Ω. The projection on the back (dotted lines) and the left (thick lines) show the evolution of the imaginary parts and real parts, respectively. The projection on the bottom shows the evolution of the eigenfrequencies in the complex plane, and EP corresponds to $\gamma/\Omega = 1$.

prepared in the ground state $|0\rangle = |^2S_{1/2}(m_J=-1/2)\rangle$, is driven to the excited state $|1\rangle = |^2D_{5/2}(m_J=+1/2)\rangle$ by a laser at wavelength 729 nm. Another laser at 854 nm induces a tunable loss γ in $|1\rangle$, by coupling $|1\rangle$ to a short-life level $|^2P_{3/2}(m_J=+3/2)\rangle$ [which decays quickly to the state $|2\rangle = |^2S_{1/2}(m_J=+1/2)\rangle$]. This configuration allows the system to exhibit coherent transition between $|0\rangle$ and $|1\rangle$, with $|1\rangle$ experiencing the required tunable loss [see Fig. 1(d)]. The effective two-level system (TLS), with coherent transition and tunable loss, is well described by the non-Hermitian Hamiltonian

$$H_{\rm eff} = \frac{\Omega}{2}\sigma_x - i\gamma|1\rangle\langle 1| \equiv H_{\mathcal{PT}} - i\frac{\gamma}{2}\mathbf{I}, \quad (1)$$

where $H_{\mathcal{PT}} = \frac{\Omega}{2}\sigma_x - i\frac{\gamma}{2}\sigma_z$ is the $\mathcal{PT}$-symmetric Hamiltonian with balanced gain and loss, $\sigma_{x(z)}$ is the Pauli matrix, and $\mathbf{I}$ is the identity operator. The spontaneous $\mathcal{PT}$ symmetry breaking in such a system then arises due to the interplay of the gain-loss rate ($\gamma/2$) and the coupling rate $\Omega/2$ [7]. As shown in Fig. 1(e), when the gain-loss rate is smaller than the coupling rate between the two states ($\gamma/\Omega < 1$), the system exhibits a real spectrum and simultaneous eigenmodes of the Hamiltonian associated with oscillatory solutions. This region is referred to as the PTS phase. Yet when the gain-loss rate is bigger than the coupling rate ($\gamma/\Omega > 1$), we call it the PTB phase where complex conjugate eigenvalues emerge, and one of the eigenmodes exponentially grows (see Supplemental Material [38]). The transition between the PTS and PTB phases takes place at an EP which emerges for $\gamma = \Omega$ [7,8].

Now we examine these predictions in our experiment. We first verify the dynamical features of this system at different phases. We initialize the system in $|0\rangle$ and tune the coupling rate $\Omega = 2\pi \times 32$ kHz at time $t = 0$, and the value of loss rate can be well controlled. We characterize the $\mathcal{PT}$-symmetry-breaking transitions by using the populations of $|0\rangle$ and the coherence in the $\{|1\rangle, |0\rangle\}$ qubit manifold, which have the following forms [38]:

$$\rho_{00}^{\mathcal{PT}}(t) = [(2\gamma^2 - \Omega^2)\cosh(\kappa t) + 2\gamma\kappa\sinh(\kappa t) - \Omega^2]/2\kappa^2, \quad (2)$$

$$\langle\sigma_y^{\mathcal{PT}}(t)\rangle = {\rm Tr}[\sigma_y\rho^{\mathcal{PT}}] = \Omega[-\gamma + \gamma\cosh(\kappa t) + \kappa\sinh(\kappa t)]/\kappa^2, \quad (3)$$

with $\kappa = \sqrt{\gamma^2 - \Omega^2}$. We see that when $\gamma > \Omega$, κ is real and the system evolves as $e^{-\kappa t}$ and $e^{\kappa t}$ (when $\kappa t \gg 1$, just

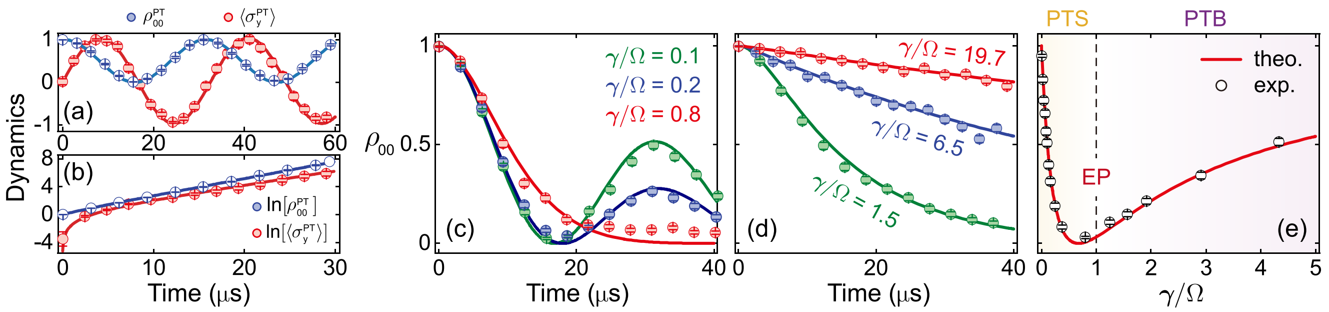

FIG. 2. (a, b) Dynamics of the $\mathcal{PT}$-symmetric system in the initial state $|0\rangle$ in the PTS phase (a) and PTB phase (b), respectively. The parameters are $\Omega = 2\pi \times 32$ kHz and $\gamma = 2\pi \times 1$ kHz (a) and $\gamma = 2\pi \times 47$ kHz (b). (c, d) The dynamics of $\rho_{00}(t)$ of the experimental TLS for two phases show oscillatory (c) to steady-state behavior (d). (e) ρ_{00} at a fixed time $t = 2\pi/\Omega$ vs the loss rate γ with $\Omega = 2\pi \times 32$ kHz. The circles or marks are the experimental data, while the lines are from the theoretical fits. The error bars are the standard deviation of the measurements.

$e^{\kappa t}$ remains) [38]. But when $\gamma < \Omega$, $\sinh(\kappa t)$ or $\cosh(\kappa t)$ corresponds to the time evolution $e^{\pm i|\kappa|t}$, featuring oscillatory evolution at angular frequency $|\kappa|$ [39].

In our experiment, directly measured quantities are the density-matrix elements of $\rho(t)$. We get the experimental data of $\rho^{\mathcal{PT}}$ from the relation $\rho^{\mathcal{PT}}(t) = e^{\gamma t}\rho(t)$, which can be easily derived from Eq. (1). The experimental results are shown in Figs. 2(a) and 2(b). When γ/Ω is tuned to the PTS phase by varying the laser power, the population and the coherence exhibit oscillation with frequency $|\kappa|$, while in the PTB phase, both the population $\rho_{00}^{\mathcal{PT}}$ and the coherence $\langle\sigma_y^{\mathcal{PT}}(t)\rangle$ increase exponentially. All the experimental results agree well with the theoretical phase diagram [38].

The $\mathcal{PT}$-symmetry-breaking phase transition can also be verified in the lossy TLS. As shown in Figs. 2(c) and 2(d), dynamical behaviors of the TLS are clearly different in PTS and PTB phases. The population of state $|0\rangle$ features decaying oscillations in the PTS phase, and meanwhile the evolution is accelerated with the increase of loss rate γ [Fig. 2(c)]. In contrast, in the PTB phase, the population of state $|0\rangle$ monotonically decays during the system evolving to a steady state, and the evolution is slowed down with the increase of loss rate γ [Fig. 2(d)]. This suggests a possible relation between $\mathcal{PT}$ symmetry and quantum Zeno effect [40–42], as proposed very recently [43–45], when the projection measurement of $|1\rangle$ is induced by extremely strong loss. This possibility will be investigated elsewhere.

We also measure the population of $|0\rangle$ at different loss rates for a fixed time $t = 2\pi/\Omega$, with $\Omega = 2\pi \times 32$ kHz, as shown in Fig. 2(e). Clearly, a turning point is observed for the population of $|0\rangle$, which can be well explained by considering the EP of H_{eff}: when the loss rate $\gamma = 0$, the populations of the two states $|0\rangle$ and $|1\rangle$ can be exchanged freely with each other; by increasing the loss rate ($\gamma < \Omega$), the state $|1\rangle$ decays to $|2\rangle$ faster via the dissipative channel and hence the population of $|0\rangle$ also decreases faster. In particular, at the EP ($\gamma = \Omega$), the coherent coupling balances with the loss of the $|1\rangle$ state, thus the population of $|0\rangle$ reaches its minimum. After this point ($\gamma > \Omega$), as the loss increases, the $|0\rangle$ state will become localized, which can be explained by quantum Zeno effect [45]. The observed phenomenon is similar to the loss-induced lasing reported in a classical system [18]. We note that $\gamma_{\min}$ in Fig. 2(e) is not exactly the EP, since the system is not at the final steady state when we do the measurement at time $t = 2\pi/\Omega$. By setting the time long enough, we can have $\gamma_{\min}$ being closer to the EP (see also Ref. [18]).

III. QUANTUM COHERENCE AT THE EP

In order to further visualize pure quantum features of the phase transition, we now introduce the order parameter by the time average of $\langle\sigma_z\rangle$ as defined in Refs. [38,46,47],

$$\Sigma_Z(\gamma) = \lim_{T\to\infty}\frac{1}{T}\int_0^T \frac{\langle\sigma_z(\gamma,t)\rangle}{\text{Tr}[\rho(\gamma,t)]}dt = \begin{cases} 0, & 0 < \gamma < \Omega, \\ -\sqrt{\gamma^2-\Omega^2}/\gamma, & \gamma \geqslant \Omega, \end{cases} \tag{4}$$

and the order parameter by the time average of $\langle\sigma_y\rangle$ [38]:

$$\Sigma_Y(\gamma) = \lim_{T\to\infty}\frac{1}{T}\int_0^T \left|\frac{\langle\sigma_y(\gamma,t)\rangle}{\text{Tr}[\rho(\gamma,t)]}\right|dt = \begin{cases} \Omega[\pi - 2\arccos(\gamma/\Omega)]/(\gamma\pi), & 0 < \gamma < \Omega, \\ \Omega/\gamma, & \gamma \geqslant \Omega. \end{cases} \tag{5}$$

We note that for open systems as the experimental TLS and the $\mathcal{PT}$ system, the traces of $\rho(t)$ and $\rho^{\mathcal{PT}}(t)$ are in general not conserved, and thus renormalization is required to study non-Hermitian dynamics [22,25,45–47]. Nevertheless, we have $\rho^{\mathcal{PT}}/\text{Tr}[\rho^{\mathcal{PT}}] = e^{-\gamma t}\rho/\text{Tr}[e^{-\gamma t}\rho] = \rho/\text{Tr}[\rho]$, hence the dynamical behaviors of $\rho(t)$ and $\rho^{\mathcal{PT}}(t)$ remain the same after the renormalization process. The order parameter $\Sigma_{Z(Y)}$, determined by γ/Ω, is independent of the initial state and clearly exhibits the transition feature for $\gamma/\Omega = 1$. We also see that at the EP, the populations of $|0\rangle$ and $|1\rangle$ are equal, i.e., the system stays in a coherent superposition state $(|0\rangle - i|1\rangle)/\sqrt{2}$ [38].

Figure 3(a) shows the experimental results about Σ_Z or the mean energy of the system. In the PTS phase, the populations of $|0\rangle$ and $|1\rangle$ are the same due to their periodic oscillations, thus leading to zero for Σ_Z; in contrast, the system can reach the steady state in the PTB phase. These results can also be observed in classical $\mathcal{PT}$ systems, since Σ_Z can only show the mean energy. In order to see true quantum $\mathcal{PT}$ features, it

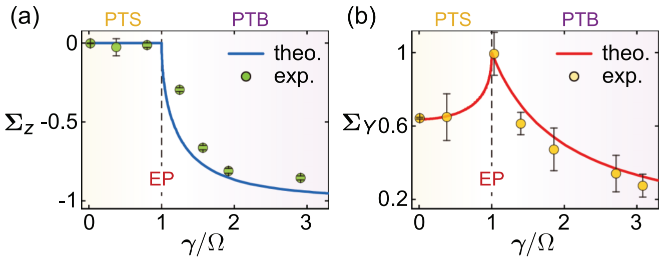

FIG. 3. The order parameters Σ_Z (a) and Σ_Y (b) vs γ, with $\Omega = 2\pi \times 32$ kHz and the initial state $|0\rangle$. The error bars indicate the estimated error from the fit to the dynamical equation for $\rho(t)$.

is necessary to study the other order parameters of the system, such as Σ_Y.

Figure 3(b) shows quantum coherence Σ_Y of the $\mathcal{PT}$-symmetric single-ion system, quantified by the modulation of nondiagonal elements of the normalized density matrix. We stress that this example of experimental observations of the order parameter Σ_Y was not given in recent quantum $\mathcal{PT}$ experiments [22,45]. We find that Σ_Y reaches its maximum when approaching the EP, i.e., quantum coherence of the $\mathcal{PT}$ system can be enhanced at the EP. This is because at the EP the balance between the loss and the coherent transition can be reached and thus enables the system to stay in coherent superposition of $|0\rangle$ and $|1\rangle$. We also note that very recently quantum discord enhancement was observed in an anti-$\mathcal{PT}$-symmetric atomic system by engineering dissipative coupling of optical channels [48].

IV. CONCLUSION

In conclusion, we have observed spontaneous $\mathcal{PT}$ symmetry breaking in a single $^{40}Ca^+$ ion. We find that when the system is steered to an EP and past it, both the mean populations of the ion states and the quantum coherence exhibit a turning point. The experimental observation of $\mathcal{PT}$ symmetry in a single trapped ion reveals the counterintuitive EP-enabled effect of quantum coherence enhancement (see also Ref. [48]). In view of the long coherence time of trapped ions, together with well-developed techniques of engineering their quantum states, our paper provides a powerful tool for exploring and utilizing true quantum EP effects at single-ion levels. In a broader view, our paper can also help to design and utilize unconventional ion-based devices, such as non-Hermitian quantum memory and EP-enhanced quantum processors or cold-ion EP clocks.

ACKNOWLEDGMENTS

The authors thank Ran Huang for helpful discussions. This work is supported by the National Basic Research Program of China under Grant No. 2016YFA0301903; the National Natural Science Foundation of China under Grants No. 11935006, No. 12074433, No. 61632021, No. 11774086, and No. 11871472; and the Natural Science Foundation of Hunan Province of China under Grant No. 2018JJ2467.

[1] C. M. Bender and S. Boettcher, Real Spectra in Non-Hermitian Hamiltonians Having $\mathcal{PT}$ Symmetry, Phys. Rev. Lett. **80**, 5243 (1998).
[2] Y. Ashida, Z. Gong, and M. Ueda, Non-Hermitian Physics, arXiv:2006.01837 (2020).
[3] R. El-Ganainy, K. G. Makris, M. Khajavikhan, Z. H. Musslimani, S. Rotter, and D. N. Christodoulides, Non-Hermitian physics and PT symmetry, Nat. Phys. **14**, 11 (2018).
[4] Ş. K. Özdemir, S. Rotter, F. Nori, and L. Yang, Parity-time symmetry and exceptional points in photonics, Nat. Mater. **18**, 783 (2019).
[5] C. M. Bender, D. C. Brody, and H. F. Jones, Complex Extension of Quantum Mechanics, Phys. Rev. Lett. **89**, 270401 (2002).
[6] C. M. Bender, Making sense of non-Hermitian Hamiltonians, Rep. Prog. Phys. **70**, 947 (2007).
[7] M.-A. Miri and A. Alù, Exceptional points in optics and photonics, Science **363**, eaar7709 (2019).
[8] F. Minganti, A. Miranowicz, R. W. Chhajlany, and F. Nori, Quantum exceptional points of non-Hermitian Hamiltonians and Liouvillians: The effects of quantum jumps, Phys. Rev. A **100**, 062131 (2019).
[9] Y.-C. Lee, M.-H. Hsieh, S. T. Flammia, and R.-K. Lee, Local $\mathcal{PT}$ Symmetry Violates the No-Signaling Principle, Phys. Rev. Lett. **112**, 130404 (2014).
[10] H. Jing, Ş. K. Özdemir, X.-Y. Lü, J. Zhang, L. Yang, and F. Nori, $\mathcal{PT}$-Symmetric Phonon Laser, Phys. Rev. Lett. **113**, 053604 (2014).
[11] C. M. Bender, D. C. Brody, H. F. Jones, and B. K. Meister, Faster than Hermitian Quantum Mechanics, Phys. Rev. Lett. **98**, 040403 (2007).
[12] U. Günther and B. F. Samsonov, Naimark-Dilated $\mathcal{PT}$-Symmetric Brachistochrone, Phys. Rev. Lett. **101**, 230404 (2008).
[13] R. El-Ganainy, K. G. Makris, D. N. Christodoulides, and Z. H. Musslimani, Theory of coupled optical PT-symmetric structures, Opt. Lett. **32**, 2632 (2007).
[14] S. Klaiman, U. Günther, and N. Moiseyev, Visualization of Branch Points in $\mathcal{PT}$-Symmetric Waveguides, Phys. Rev. Lett. **101**, 080402 (2008).
[15] L. Xiao, T. Deng, K. Wang, G. Zhu, Z. Wang, W. Yi, and P. Xue, Non-Hermitian bulk-boundary correspondence in quantum dynamics, Nat. Phys. **16**, 761 (2020).
[16] L. Feng, Z. J. Wong, R.-M. Ma, Y. Wang, and X. Zhang, Single-mode laser by parity-time symmetry breaking, Science **346**, 972 (2014).
[17] H. Hodaei, M.-A. Miri, M. Heinrich, D. N. Christodoulides, and M. Khajavikhan, Parity-time–symmetric microring lasers, Science **346**, 975 (2014).
[18] A. Guo, G. J. Salamo, D. Duchesne, R. Morandotti, M. Volatier-Ravat, V. Aimez, G. A. Siviloglou, and D. N. Christodoulides, Observation of $\mathcal{PT}$-Symmetry Breaking in Complex Optical Potentials, Phys. Rev. Lett. **103**, 093902 (2009).
[19] B. Peng, Ş. K. Özdemir, S. Rotter, H. Yilmaz, M. Liertzer, F. Monifi, C. M. Bender, F. Nori, and L. Yang, Loss-

induced suppression and revival of lasing, Science **346**, 328 (2014).

[20] W. Chen, Ş. K. Özdemir, G. Zhao, J. Wiersig, and L. Yang, Exceptional points enhance sensing in an optical microcavity, Nature (London) **548**, 192 (2017).

[21] H. Hodaei, A. U. Hassan, S. Wittek, H. Garcia-Gracia, R. El-Ganainy, D. N. Christodoulides, and M. Khajavikhan, Enhanced sensitivity at higher-order exceptional points, Nature (London) **548**, 187 (2017).

[22] Y. Wu, W. Liu, J. Geng, X. Song, X. Ye, C.-K. Duan, X. Rong, and J. Du, Observation of parity-time symmetry breaking in a single-spin system, Science **364**, 878 (2019).

[23] S. Scheel and A. Szameit, $\mathcal{PT}$-symmetric photonic quantum systems with gain and loss do not exist, Europhys. Lett. **122**, 34001 (2018).

[24] L. Xiao, X. Zhan, Z. H. Bian, K. K. Wang, X. Zhang, X. P. Wang, J. Li, K. Mochizuki, D. Kim, N. Kawakami, W. Yi, H. Obuse, B. C. Sanders, and P. Xue, Observation of topological edge states in parity-time-symmetric quantum walks, Nat. Phys. **13**, 1117 (2017).

[25] M. Naghiloo, M. Abbasi, Y. N. Joglekar, and K. W. Murch, Quantum state tomography across the exceptional point in a single dissipative qubit, Nat. Phys. **15**, 1232 (2019).

[26] Y. Wang, M. Um, J. Zhang, S. An, M. Lyu, J. N. Zhang, L. M. Duan, D. Yum, and K. Kim, Single-qubit quantum memory exceeding ten-minute coherence time, Nat. Photonics **11**, 646 (2017).

[27] B. Tabakov, J. Bell, D. F. Bogorin, B. Bonenfant, P. Cook, L. Disney, T. Dolezal, J. P. O'Reilly, J. Phillips, K. Poole, L. Wessing, and K.-A. Brickman-Soderberg, Towards using trapped ions as memory nodes in a photon-mediated quantum network, Proc. SPIE **10660**, 106600L (2018).

[28] D. Kielpinski, V. Meyer, M. A. Rowe, C. A. Sackett, W. M. Itano, C. Monroe, and D. J. Wineland, A decoherence-free quantum memory using trapped ions, Science **291**, 1013 (2001).

[29] C. R. Monroe and D. J. Wineland, Quantum computing with ions, Sci. Am. **299**, 64 (2008).

[30] T. Brydges, A. Elben, P. Jurcevic, B. Vermersch, C. Maier, B. P. Lanyon, P. Zoller, R. Blatt, and C. F. Roos, Probing Rényi entanglement entropy via randomized measurements, Science **364**, 260 (2019).

[31] J. Zhang, G. Pagano, P. W. Hess, A. Kyprianidis, P. Becker, H. Kaplan, A. V. Gorshkov, Z. X. Gong, and C. Monroe, Observation of a many-body dynamical phase transition with a 53-qubit quantum simulator, Nature (London) **551**, 601 (2017).

[32] B. P. Lanyon, C. Hempel, D. Nigg, M. Müller, R. Gerritsma, F. Zähringer, P. Schindler, J. T. Barreiro, M. Rambach, G. Kirchmair, M. Hennrich, P. Zoller, R. Blatt, and C. F. Roos, Universal digital quantum simulation with trapped ions, Science **334**, 57 (2011).

[33] R. Blatt and C. F. Roos, Quantum simulations with trapped ions, Nat. Phys. **8**, 277 (2011).

[34] C. Schneider, D. Porras, and T. Schaetz, Experimental quantum simulations of many-body physics with trapped ions, Rep. Prog. Phys. **75**, 024401 (2012).

[35] T. Rosenband, D. B. Hume, P. O. Schmidt, C. W. Chou, A. Brusch, L. Lorini, W. H. Oskay, R. E. Drullinger, T. M. Fortier, J. E. Stalnaker, S. A. Diddams, W. C. Swann, N. R. Newbury, W. M. Itano, D. J. Wineland, and J. C. Bergquist, Frequency ratio of Al^+ and Hg^+ single-ion optical clocks; metrology at the 17th decimal place, Science **319**, 1808 (2008).

[36] N. Huntemann, M. Okhapkin, B. Lipphardt, S. Weyers, C. Tamm, and E. Peik, High-Accuracy Optical Clock Based on the Octupole Transition in $^{171}Yb^+$, Phys. Rev. Lett. **108**, 090801 (2012).

[37] T. Baumgratz, M. Cramer, and M. B. Plenio, Quantifying Coherence, Phys. Rev. Lett. **113**, 140401 (2014).

[38] See Supplemental Material at http://link.aps.org/supplemental/10.1103/PhysRevA.103.L020201 for additional details, which includes Refs. [8,39,46,47].

[39] K. Macieszczak, M. Guţă, I. Lesanovsky, and J. P. Garrahan, Towards a Theory of Metastability in Open Quantum Dynamics, Phys. Rev. Lett. **116**, 240404 (2016).

[40] E. W. Streed, J. Mun, M. Boyd, G. K. Campbell, P. Medley, W. Ketterle, and D. E. Pritchard, Continuous and Pulsed Quantum Zeno Effect, Phys. Rev. Lett. **97**, 260402 (2006).

[41] M. C. Fischer, B. Gutiérrez-Medina, and M. G. Raizen, Observation of the Quantum Zeno and Anti-Zeno Effects in an Unstable System, Phys. Rev. Lett. **87**, 040402 (2001).

[42] Y. S. Patil, S. Chakram, and M. Vengalattore, Measurement-Induced Localization of an Ultracold Lattice Gas, Phys. Rev. Lett. **115**, 140402 (2015).

[43] J. Li, T. Wang, L. Luo, S. Vemuri, and Y. N. Joglekar, Unification of quantum Zeno-anti Zeno effects and parity-time symmetry breaking transitions, arXiv:2004.01364 (2020).

[44] T. Chen, W. Gou, D. Xie, T. Xiao, W. Yi, J. Jing, and B. Yan, Quantum Zeno effects across a parity-time symmetry breaking transition in atomic momentum space, arXiv:2009.01419 (2020).

[45] J. Li, A. K. Harter, J. Liu, L. De Melo, Y. N. Joglekar, and L. Luo, Observation of parity-time symmetry breaking transitions in a dissipative Floquet system of ultracold atoms, Nat. Commun. **10**, 855 (2019).

[46] D. C. Brody and E.-M. Graefe, Mixed-State Evolution in the Presence of Gain and Loss, Phys. Rev. Lett. **109**, 230405 (2012).

[47] K. Kawabata, Y. Ashida, and M. Ueda, Information Retrieval and Criticality in Parity-Time-Symmetric Systems, Phys. Rev. Lett. **119**, 190401 (2017).

[48] W. Cao, X. Lu, X. Meng, J. Sun, H. Shen, and Y. Xiao, Reservoir-Mediated Quantum Correlations in Non-Hermitian Optical System, Phys. Rev. Lett. **124**, 030401 (2020).